

# Balance between Exocytosis and Endocytosis Determines the Efficacy of Sterol-Targeting Antibiotics

Shinichi Nishimura,<sup>1,\*</sup> Masato Tokukura,<sup>1</sup> Junko Ochi,<sup>1</sup> Minoru Yoshida,<sup>2</sup> and Hideaki Kakeya<sup>1,\*</sup>

<sup>1</sup>Division of Bioinformatics and Chemical Genomics, Department of System Chemotherapy and Molecular Sciences, Graduate School of Pharmaceutical Sciences, Kyoto University, Kyoto 606-8501, Japan

<sup>2</sup>Chemical Genomics Research Group, RIKEN Center for Sustainable Resource Science, Wako, Saitama 351-0198, Japan

\*Correspondence: [nshin@pharm.kyoto-u.ac.jp](mailto:nshin@pharm.kyoto-u.ac.jp) (S.N.), [scseigyo-hisyo@pharm.kyoto-u.ac.jp](mailto:scseigyo-hisyo@pharm.kyoto-u.ac.jp) (H.K.)

<http://dx.doi.org/10.1016/j.chembiol.2014.10.014>

## SUMMARY

Antifungals targeting membrane ergosterol are longstanding, yet indispensable drugs in clinical use. However, the mechanisms by which the cellular membrane domains recognized by these antibiotics are generated remain largely unknown. Here, we demonstrate that the balance between endocytosis and exocytosis in membrane trafficking is a critical factor in the action of sterol-targeting antibiotics. When fission yeast cells were treated with manumycin A, cellular binding and the action of the antifungals filipin, amphotericin B, and theonellamides, all of which are ergosterol-binders, were abolished. Additionally, manumycin A treatment attenuated Cdc42 activity and inhibited exocytosis, while endocytosis was only moderately suppressed. Similar defects in membrane trafficking could be reproduced by heat shock and genetic perturbation, which also abolished the action of the antibiotics. We propose that exocytosis and endocytosis respectively supply and internalize the specific plasma membrane domains recognized by sterol-targeting antibiotics.

## INTRODUCTION

The cell membrane serves as a physical barrier that defines the cell boundary and segregates the interior into distinct compartments, each performing a specialized function. Among the many lipid constituents of cell membranes, sterols are unique in that they are major regulators of membrane fluidity and thickness and contribute to the formation of specific membrane microdomains (Simons and Ikonen, 1997). Additionally, sterols are medically important molecules often targeted by antibiotics and toxins. Using artificial membranes, many studies have been carried out to gain insights into the action of sterol-targeting exogenous molecules. However, as yet, little is known about how antibiotics recognize the cellular membrane, and how the corresponding membrane domains are generated in the cell (Bolard, 1986; Gray et al., 2012). Cellular membranes

are highly complex; it is therefore imperative to use the right model organism with clear-cut phenotypes to elucidate the basic mechanisms behind the construction of the living cell membrane.

The fission yeast *Schizosaccharomyces pombe* is a rod-shaped unicellular organism that grows by length extension at the cell tips, where actin patches, glucan synthases, and the processes of exocytosis and endocytosis are all concentrated (Hayles and Nurse, 2001). Sterol-rich domains in the plasma membrane have also been detected at the growing cell tips (Wachtler et al., 2003). Most of the components located at the cell tips during interphase, including these sterol-rich plasma membrane domains, are recruited to the site of cytokinesis for equal distribution upon cell division. Since the polarity of sterol-rich membrane domains in *S. pombe* cells can be clearly visualized using sterol probes and fluorescence microscopy (Nishimura et al., 2010; Wachtler et al., 2003), *S. pombe* is an excellent model organism for investigating the physical and biological nature of sterol-rich membrane domains. The polarized distribution of these domains is regulated in a cell cycle-dependent manner (Wachtler et al., 2003) and has been shown to require normal actin cytoskeleton organization (Codlin et al., 2008; Takeda et al., 2004), myosin type I (Myo1) protein (Takeda and Chang, 2005), and Cdc15, a contractile ring protein (Takeda et al., 2004).

In addition to the cytoskeletal machinery, the functional secretory pathway was also shown to be necessary for sterol-rich membrane domain distribution; in cell-cycle mutant *cdc25-22* cells, brefeldin A (BFA), an inhibitor of ER-to-Golgi transport (Graham et al., 1993), inhibited the appearance of sterol-rich domains (Wachtler et al., 2003). However, in wild-type cells, BFA treatment yielded rather bright fluorescent signals that lost polarity, raising the question of whether the functional secretory pathway alone is sufficient for generating polarized sterol localization (Figure S1A available online).

During the course of screening for chemical modulators of the action of membrane-targeting antibiotics, we found that manumycin A (manu-A) inhibited the binding of sterol-targeting antibiotics to fission yeast cells. Here, using manu-A as a chemical genetics tool, we demonstrate that the balance between exocytosis and endocytosis is critical for generating the membrane domains recognized by sterol-targeting antibiotics.

## RESULTS AND DISCUSSION

### Manu-A Abolishes the Cellular Binding of Sterol-Targeting Antibiotics

Sterol-rich domains in the plasma membrane can be visualized with filipin, a polyene antibiotic that exhibits fluorescence upon binding to membrane sterols (Drabikowski et al., 1973). To investigate how cellular membranes are recognized by sterol-targeting antibiotics, we tested a set of chemicals for their effect on filipin staining. We found that when cells were pretreated with manu-A (see structure in Figure 1A), the fluorescent signal from filipin was absent (Figure 1B). There are two possible mechanisms for this phenomenon: manu-A might quench the fluorescence of the filipin-sterol complexes, or it might sequester sterols, thereby hampering the formation of the filipin-sterol complexes. To investigate these possibilities, we tested the effect of manu-A on other sterol-targeting antibiotics. First, we tested amphotericin B (AmB), another polyene antibiotic that is commonly prescribed as an ergosterol-targeting antifungal drug (Volmer et al., 2010). AmB is known to induce large vacuoles in yeast cells, probably as a consequence of binding to ergosterol (Bhuiyan et al., 1999). However, this morphological change was suppressed when the cells were pretreated with manu-A (Figure 1C). Notably, the toxicity of filipin and AmB were also attenuated (Figure 1D). In fission yeast cells, filipin showed toxicity at 2  $\mu\text{g/ml}$  and partially inhibited growth of the cells at 1  $\mu\text{g/ml}$ . In the presence of manu-A, growth inhibition by filipin (1  $\mu\text{g/ml}$ ) was not observed, although it must be noted that cell growth was attenuated by manu-A across all filipin concentrations. The mitigating effect of manu-A on AmB toxicity was more distinct, as the minimum inhibitory concentration (MIC value) of AmB doubled in the presence of manu-A.

Next, we examined theonellamides (TNMs), bicyclic peptides isolated from marine sponges (Matsunaga and Fusetani, 1995; Matsunaga et al., 1989) that target membrane sterols (Espirito et al., 2013). TNM fluorescent derivatives, such as TNM-amino-methylcoumarin acetate (AMCA), specifically recognize  $3\beta$ -hydroxysterols. These fluorescent derivatives can therefore act as markers of  $3\beta$ -hydroxysterols in both yeast (Ho et al., 2009; Nishimura et al., 2010) and cultured mammalian cells (Nishimura et al., 2013). TNM-AMCA treatment of the fission yeast cells exhibited polarized staining similar to that obtained with filipin, and this staining was also inhibited by pretreatment with manu-A (Figure 1E). Treatment of fission yeast cells with TNMs induces abnormal cell wall morphology (Nishimura et al., 2010). Consistent with the inhibition of the cellular binding of TNM-AMCA by manu-A, this abnormal cell wall phenotype was not observed following pretreatment with manu-A (data not shown). Additionally, growth inhibition by TNM-A was also attenuated (Figure 1D), and manu-A quadrupled the MIC value of this compound. Because filipin, AmB, and TNMs belong to different chemical classes based on their structure (Figure S2), the effect of manu-A is unlikely to be dependent on the chemical properties of the antibiotics. It is unlikely that the fluorescence of the filipin-sterol complexes was directly quenched by manu-A. Instead, it is likely that manu-A treatment sequesters antibiotic-targeted ergosterol molecules in the plasma membrane using as yet unknown mechanisms.

Manu-A was originally isolated from *Streptomyces parvulus* (Zeeck et al., 1987). This metabolite has been reported to inhibit several enzymes including caspase I (Tanaka et al., 1996) and neutral sphingomyelinase (Arenz et al., 2001), and protein farnesyltransferase (FTase) (Hara et al., 1993). It has also been observed to inhibit protein FTase in the budding yeast, *Saccharomyces cerevisiae* (Hara et al., 1993). We therefore examined the possibility that FTase inhibition is responsible for the effects of manu-A observed in *S. pombe*. Protein FTase consists of  $\alpha$  and  $\beta$  subunits encoded by the *cwp1* and *cwp2* genes, respectively. FTase activity was abolished in cells lacking the *cwp1* gene (Yang et al., 2000), however, sterol-rich membrane domains were still observed to localize in a polarized manner, although polarity in the cell shape was severely reduced (Figure 1F) (Ma et al., 2006). Additionally, the sterol-rich domains of these mutant cells disappeared after treatment with manu-A. We also examined the *css1* gene, which encodes inositol phosphosphingolipid phospholipase C, a yeast counterpart of mammalian sphingomyelinase. Manu-A has been reported to inhibit neutral sphingomyelinase (Arenz et al., 2001). Sphingomyelinase catalyzes the hydrolysis of sphingomyelin to produce ceramide, which is required for membrane budding in liposomes and exocytosis in mammalian cells (Trajkovic et al., 2008). However, *css1* mutant cells did not reproduce the phenotype of manu-A treatment (Figure S3A). These results indicated that protein FTase and inositol phosphosphingolipid phospholipase C do not mediate the effect of manu-A on the plasma membrane.

### Sterol Levels and Sterol-Rich Membrane Domains

The disappearance of sterol-rich domains from the plasma membrane can be caused by a decrease in sterol levels. We therefore measured the amount of ergosterol present in cells subsequent to treatment with manu-A, under the following two conditions. When cells were cultivated in a rich medium containing manu-A (1  $\mu\text{g/ml}$ ), the ergosterol level decreased to  $77.7 \pm 6.0\%$  and no filipin signal was detected (Figure 1B). In contrast, when cells were cultivated in a synthetic medium, a lower concentration of manu-A (0.1  $\mu\text{g/ml}$ ) decreased the ergosterol level to a similar level of  $75.6 \pm 2.7\%$ , although the filipin signal was still observed (Figure S3B). These results revealed that the amount of ergosterol present could not be correlated to the presence or absence of sterol-rich domains in the plasma membrane. We next compared the kinetics of the effect of manu-A and terbinafine, a potent inhibitor of squalene epoxidase, a requisite enzyme for ergosterol biosynthesis (Figures S3C and S3D). Compared with manu-A, a longer incubation period (more than 5 h) with terbinafine was required before the sterol-rich membrane domains were observed to disappear. These results suggested that a decrease in ergosterol was not responsible for the disappearance of sterol-rich membrane domains in the presence of manu-A. The decreased ergosterol levels affected by manu-A may be a result of feedback regulation following dysregulation of membrane trafficking (as discussed further below). As a case in point, cells lacking the *apm1* gene, which encodes the AP-1 adaptor complex  $\mu$  subunit involved in vesicle-mediated transport, are known to contain only about 50% of ergosterol due to an unknown mechanism (Fang et al., 2012).

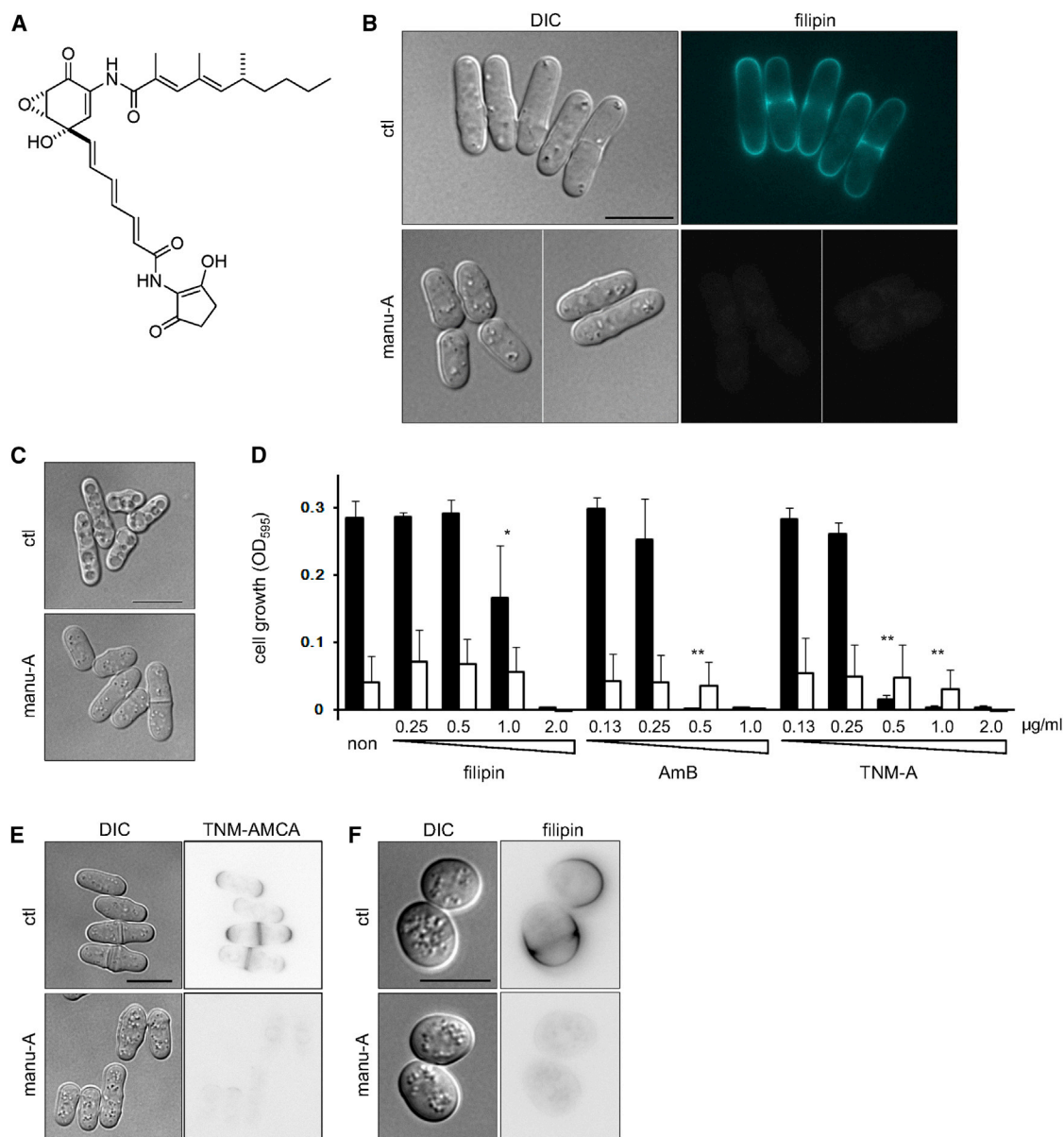


**Figure 1. Manu-A Abolishment of the Binding and Effect of Sterol-Binding Antibiotics**

(A) Chemical structure of manu-A.

(B) Sterol-rich plasma membrane domains of fission yeast cells. Domains were visualized with filipin (upper right hand panel). Manu-A treatment (1  $\mu\text{g/ml}$ ) for 1 hr abolished the fluorescent signal of filipin binding (lower right hand panel).

(C) Cellular effect of AmB. Cells were treated with AmB (1  $\mu\text{g/ml}$ ) for 1 hr in the presence or absence of manu-A (1  $\mu\text{g/ml}$ ) and observed under microscopy.

(D) Effect of manu-A on the growth inhibition exerted by antibiotics. Yeast cells were incubated with sterol-targeting antibiotics in the presence (white) or absence (black) of manu-A (0.5  $\mu\text{g/ml}$ ) for 26 hr. Data represent the mean  $\pm$  SD,  $n = 3-4$ . Statistical significance of  $p < 0.05$  (\*) and  $p < 0.01$  (\*\*) were determined by t test, calculated using cell growth values normalized using optical density of the cultures in the absence of manu-A.

(E) Binding of TNM-AMCA in the presence of manu-A. Cells were incubated with or without manu-A (1  $\mu\text{g/ml}$ ) for 1 hr, and then stained with TNM-AMCA (1  $\mu\text{g/ml}$ ) for 1 hr.

(F) Sterol-rich domains in *cyp1 $\Delta$*  cells. The domains were visualized with filipin in the presence or absence of manu-A (1  $\mu\text{g/ml}$ ). Scale bars, 10  $\mu\text{m}$ . Control (ctl), differential interference contrast microscopy (DIC).

### Relationship between Manu-A and Cdc42

Sterol localization is controlled in a cell cycle-dependent manner (Wachtler et al., 2003); we therefore hypothesized that the effect of manu-A on the plasma membrane would correlate with its cell growth inhibitory activity. To identify the genes involved in

the action of manu-A, we conducted a genome-wide screen using a decreased abundance by mRNA perturbation (DAmP) strain collection of the budding yeast *Saccharomyces cerevisiae* (Breslow et al., 2008; Yan et al., 2008). DAmP acts by destabilizing mRNA transcripts through the integration of an

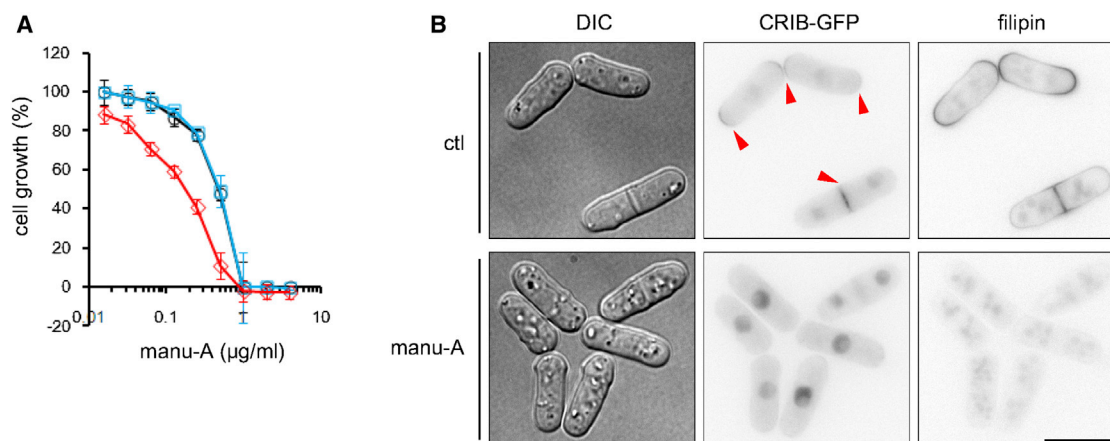


**Figure 2. Relationship between Cdc42 and Manu-A**

(A) Effect of Cdc42 expression levels on manu-A sensitivity. Cells containing mock vectors (black), cells overexpressing wild-type Cdc42 (blue), or the dominant-negative form, Cdc42-T17N (red), were cultured in the presence of manu-A. Cell growth was measured after 48 hr incubation. Data represent the mean  $\pm$  SD,  $n = 4$ .

(B) Cellular localization of activated Cdc42 (detected using CRIB-GFP) and sterol-rich membrane domains (detected using filipin). Cells treated with or without manu-A (1  $\mu$ g/ml) for 1 hr were observed under fluorescent microscopy. Arrowheads indicate the colocalization of CRIB-GFP and filipin signals. Scale bar, 10  $\mu$ m.

antibiotic-selectable marker into the 3' untranslated regions of genes of interest, thereby yielding hypomorphic alleles (Muhlrad and Parker, 1999). Genes involved in the mode of action of a bioactive compound can then be identified by screening DAmP strain collections for strains that are sensitive to the compound (Breslow et al., 2008; Yan et al., 2008).

The growth of the budding yeast cells was observed to be sensitive to manu-A (Figure S4A). After screening 878 haploid DAmP strains, we identified 28 genes for which downregulation conferred increased sensitivity to manu-A (Figures S4A–S4C). Among these, we found several genes involved in membrane trafficking: *SEC31*, which encodes a component of the COPII vesicle coat required for vesicle formation in ER-to-Golgi transport; and *PAN1*, which encodes a protein that associates with actin patches and promotes protein-protein interactions essential for endocytosis. *ERG8*, an essential gene for the biosynthesis of isoprenoids and ergosterol, was also identified. Notably, *CDC24*, which encodes a guanosine diphosphate-guanosine triphosphate (GTP) exchange factor for Cdc42, was similarly identified as a sensitive DAmP mutant (Park and Bi, 2007). Cdc42 is known to regulate the polarization of the actin cytoskeleton and membrane trafficking toward the sites of cell growth (Park and Bi, 2007; Perez and Rincón, 2010).

These results led us to hypothesize that manu-A perturbs Cdc42, which in turn effects the formation of sterol-rich membrane domains. To test whether manu-A targets the Cdc42 pathway in fission yeast, we first examined the effect of overexpression of Cdc42 on the growth inhibitory activity of manu-A. Overexpression of wild-type Cdc42 had no effect, whereas cells expressing the dominant-negative form of Cdc42 became more sensitive to manu-A compared with cells containing mock vectors (Figure 2A). We next examined the activity of Cdc42 using a fluorescent fusion protein called Cdc42/Rac interactive binding peptide-green fluorescent protein (CRIB)-GFP, which specifically binds to activated, GTP-bound Cdc42 (Tatebe et al., 2008).

In wild-type cells, CRIB-GFP signal was concentrated at the growing cell tips during interphase and around the division plane during mitosis (Figure 2B). After the addition of manu-A, cortical GFP signal was barely detectable, indicating that Cdc42 was inactivated. In contrast, cortical localization visualized using GFP-Cdc42 fusion protein was not abolished completely, and the prenylation status of Cdc42 protein appeared unaffected by manu-A (Figures S4D and S4E). Together, these results suggested that the Cdc42 activation pathway is targeted by manu-A in fission yeast cells.

### Inhibition of Exocytosis by Manu-A

In fission yeast cells, Cdc42 regulates the actin cytoskeleton (Martin et al., 2007; Rincón et al., 2009) and multiple membrane trafficking events (Estravis et al., 2011). Since Cdc42 was downregulated by manu-A, we next investigated whether the effect of manu-A was mediated through the disorganization of the actin cytoskeleton and/or dysregulation of membrane trafficking. In fission yeast cells, the actin cytoskeleton consists of actin cables, actin patches, and a contractile ring during vegetative growth (Kovar et al., 2011). Cells treated with manu-A exhibited apparently delocalized actin patches with randomly localized actin cables, indicating that cells lost polarity in actin structures in the presence of manu-A (Figure S5A). However, genetic perturbation of the actin cytoskeleton organization did not result in a similar phenotype; when temperature-sensitive *cps8-188* cells were left at the restriction temperature, the fluorescent signal of filipin became delocalized and distributed over the plasma membrane (Codlin et al., 2008). Furthermore, the effect of manu-A on cell growth was almost indistinguishable between actin mutant cells and wild-type cells (Figure 3A). These results indicated that the effect of manu-A on the plasma membrane was not exerted through disorganization of the actin cytoskeleton.

Next, we investigated the relationship between manu-A and membrane trafficking. A terminal phenotype of a thermosensitive



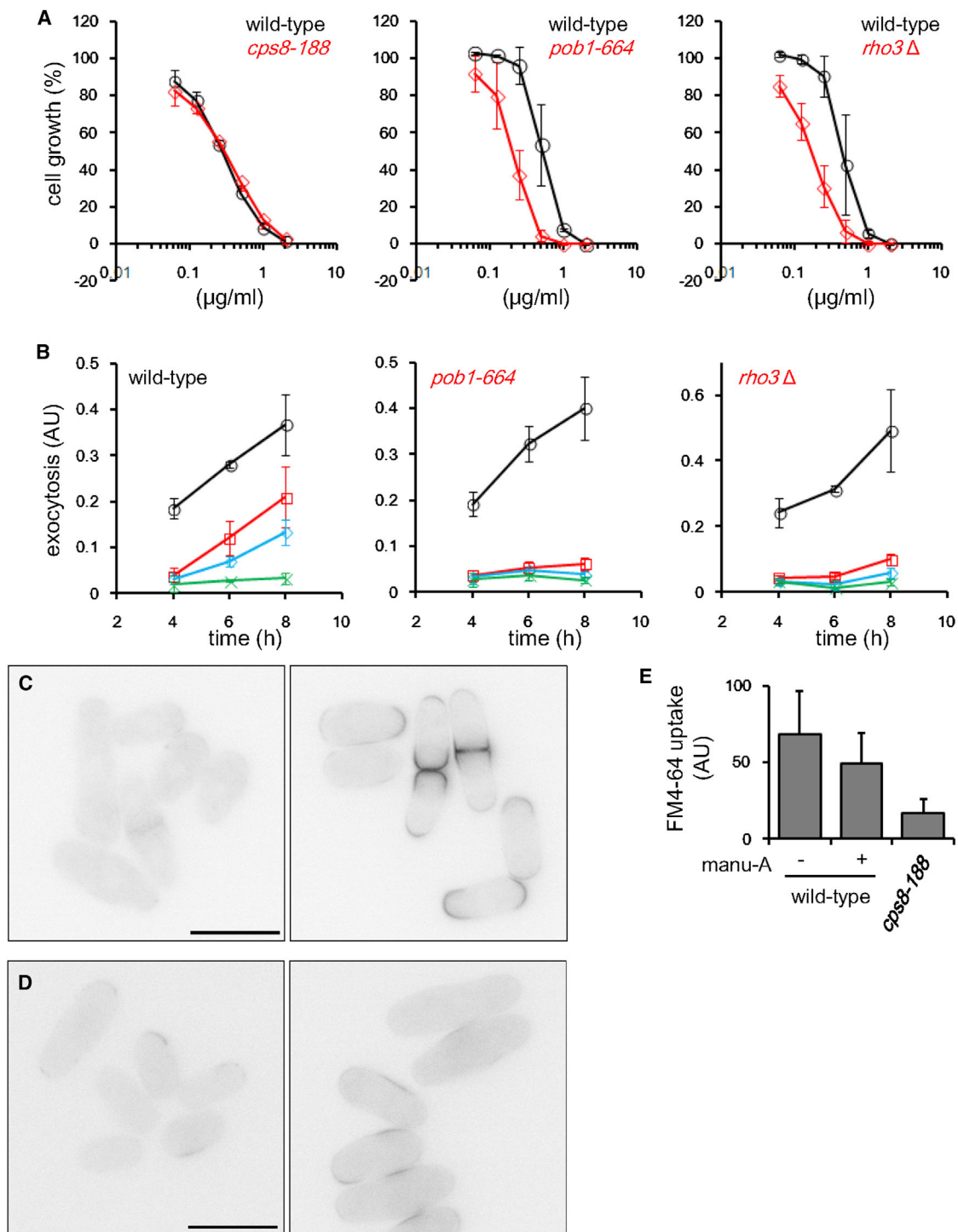


**Figure 3. Effect of Manu-A on Cell Growth, Exocytosis, and Endocytosis**

(A) Growth inhibition of mutant cells by manu-A. Growth of *cps8-188* cells (27°C for 24 hr), *pob1-664* cells (30°C for 26 hr), and *rho3Δ* cells (30°C for 26 hr) in the presence of manu-A was compared with that of wild-type cells.

(B) Exocytosis inhibition by manu-A. Activity of secreted acid phosphatase from wild-type, *pob1* mutant, and *rho3* deletion cells in the presence of manu-A was measured. Acid phosphatase activity was normalized with cell density. Cells were cultivated at 27°C and at various manu-A concentrations: 0 (black), 0.05 (red), 0.1 (blue), and 0.5 (green) μg/ml.

(C) Reappearance of sterol-rich membrane domains after treatment with a low concentration of manu-A. Manu-A (0.05 μg/ml) was added to the cells in EMMP, followed by visualization of sterol-rich membrane domains using filipin. Fluorescent images after 1 hr treatment (left) and 5 hr treatment (right) are shown.

(legend continued on next page)

strain of *cdc42* is a defect in exocytosis (Estravís et al., 2011). To test the possibility that manu-A inhibits exocytosis, we measured the secretion of acid phosphatase, a protein marker of exocytosis (Wang et al., 2002). When cells were exposed to manu-A, secretion of acid phosphatase was inhibited in a dose-dependent manner (Figure 3B). The effective concentration was comparable to that necessary for inhibiting the cellular binding of antibiotics. Many protein factors have been reported to be involved in exocytosis; for example, Pob1, which is involved in polarized growth; and a small GTPase, Rho3, which regulates cell separation. Although the precise molecular mechanism remains to be clarified, introducing mutations in the *pob1* gene (*pob1-664*; see Nakano et al., 2011) or deletion of the *rho3* gene (*rho3Δ*; see Wang et al., 2003) have been shown to decrease secretion resulting from exocytosis. When we challenged these mutant cells with manu-A, exocytosis was suppressed at lower manu-A concentrations compared with the wild-type cells (Figure 3B); moderate inhibition was observed in wild-type cells at 0.05–0.1 μg/ml, whereas exocytosis was almost completely inhibited in the mutant cells at a concentration as low as 0.05 μg/ml. Additionally, manu-A more efficiently inhibited cell growth of the exocytosis mutant cells compared with the wild-type cells (Figure 3A). In contrast, exocytosis of actin mutant cells was not more sensitive to manu-A compared with wild-type cells (Figure S5B). These results showed that the observed cell growth inhibition by manu-A was, at least in part, a result of the suppression of exocytosis, which in turn led to the loss of cellular binding of sterol-targeting antibiotics.

### Inhibition of Exocytosis Leads to the Disappearance of Sterol-Rich Plasma Membrane Domains

Treatment of wild-type cells with manu-A at a low concentration (0.05 μg/ml) inhibited exocytosis, but this inhibition was gradually released (Figure 3B). If exocytosis supplies sterol-rich membrane domains, recovery of exocytosis should lead to the recovery of these membrane domains. We indeed observed this using filipin staining of cells treated with a low concentration of manu-A; although treating wild-type cells with 0.05 μg/ml manu-A for 1 hr initially abolished the filipin signal, the same signal reappeared 5 hr later (Figure 3C). In contrast, when higher concentrations of manu-A were used, e.g., 0.5 μg/ml, the filipin signal was only barely detectable 6 hr following the initial treatment (Figure S6).

The exocytosis activities of the *pob1* mutant and *rho3Δ* cells were found to be more sensitive to manu-A than that of wild-type cells. We examined recovery of the filipin signal in these mutant cells and found that in *pob1* mutant cells, recovery of the filipin signal was not observed (Figure 3D). Similarly, the lack of *rho3* protein significantly perturbed the signal recovery and only weak and irregular filipin staining was observed (Figure 3D). Together, these results indicate that manu-A inhibits exocytosis, the route by which the

sterol-rich membrane domains are supplied to the plasma membrane.

### Endocytosis Is Requisite for the Disappearance of Sterol-Rich Plasma Membrane Domains

Manu-A inhibits exocytosis, and this inhibition appears to abolish the production of sterol-rich membrane domains in the plasma membrane. However, inhibition of the supply of sterol-rich membrane domains may not be sufficient for the complete abolishment of antibiotic action, since certain portions of the sterol-rich membrane domains should already have been delivered to the plasma membrane prior to the addition of manu-A. This suggested the possibility that endocytosis could selectively internalize these domains, a process that may not be inhibited by manu-A. Our next experiments therefore tested the effect of manu-A on endocytosis.

In fission yeast cells, the fluorescent styryl dye FM4-64 is used as a marker for the endocytic pathway, as FM4-64 is internalized by endocytosis at the growing areas of the cell and is subsequently transported to the vacuolar membrane (Gachet and Hyams, 2005). Within 30 min of the addition of FM4-64, intermediate compartments became stained despite the presence of manu-A (although the dye intensity was slightly decreased), indicating that endocytosis was uninhibited by manu-A (Figure 3E). This analysis suggested that manu-A did not inhibit the uptake of plasma membrane domains, despite inhibiting the supply thereof to the membrane and consequently inhibiting the generation of sterol-rich membrane domains. This corroborates a previous finding in budding yeast, where secretory vesicles were observed to be enriched in ergosterol and sphingolipids (Klemm et al., 2009).

We also tested the effect of BFA on FM4-64 incorporation. Cells treated with BFA showed intense and nonpolarized filipin signal (Figure S1A). If the balance of exocytosis and endocytosis determines the binding of sterol-targeting antibiotics, BFA should have the opposite effect of manu-A. As expected, BFA suppressed incorporation of FM4-64 (Figure S1C). This was consistent with a previous report demonstrating BFA inhibition of FM4-64 incorporation at the equatorial region in dividing cells (Gachet and Hyams, 2005). In contrast, the secretion of acid phosphatase was unaffected (Figure S1B). This result indicated that the continuing export and simultaneous inhibition of the uptake of membrane domains by BFA led to the accumulation of sterols in the plasma membrane as visualized with filipin staining.

### Heat Shock Leads to the Disappearance of Sterol-Rich Plasma Membrane Domains

Heat shock treatment induces a variety of cellular responses to adapt to this condition (Verghese et al., 2012). We found that sterol-rich membrane domains are also sensitive to heat shock, as the filipin signal in wild-type cells was significantly decreased after the temperature was shifted from 27°C to 37°C (Figure 4A). This response was transient and the sterol-rich membrane

(D) Lack of reappearance of sterol-rich membrane domains in mutant cells. *pob1-664* (left) and *rho3Δ* cells (right) were treated with 0.05 μg/ml manu-A and stained with filipin after 5 hr.

(E) Effect of manu-A on endocytosis. Uptake of FM4-64 by wild-type cells was observed after treatment with DMSO (0.1%) or manu-A (1 μg/ml) for 1 hr. FM4-64 was added to the culture and cells were observed under fluorescence microscopy. Uptake of FM4-64 was calculated after 0.5 hr. In a control experiment, *cps8-188* cells were shifted to the restriction temperature (37°C) for 1 hr, followed by FM4-64 treatment and observation of FM4-64 uptake.

In (A) and (B), data represent the mean ± error bars, SD, n = 3. In (E), data represent the mean ± error bars, SE, n = 3.

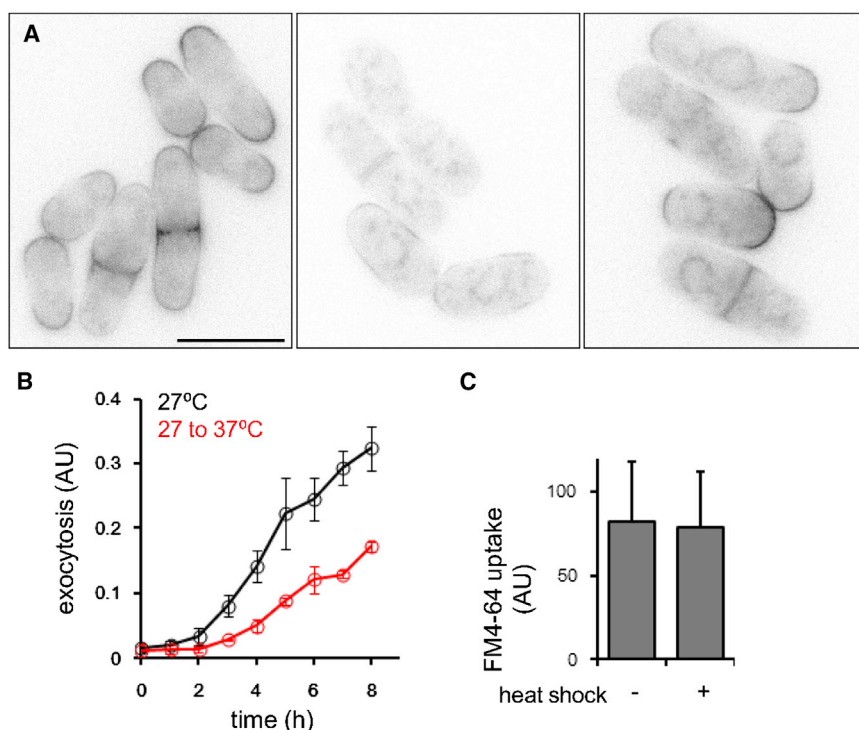


**Figure 4. Transient Disappearance of Sterol-Rich Plasma Membrane Domains following Heat Shock**

(A) Disappearance and reappearance of sterol-rich plasma membrane domains following heat shock treatment. Wild-type cells in YE5S were shifted from 27°C (left) to 37°C for 1 hr (middle) and 5 hr (right), and the presence of sterol-rich membrane domains was visualized using filipin. Scale bar, 10  $\mu$ m.

(B) Kinetics of exocytosis after heat shock. Cells were cultured at 27°C (black) or shifted from 27°C to 37°C (red) at time 0. Activity of secreted acid phosphatase was measured and normalized with cell density. Data represent the mean  $\pm$  SD,  $n = 3$ .

(C) Effect of heat shock on endocytosis. Wild-type cells in YE5S were shifted from 27°C (left) to 37°C for 1 hr, and uptake of FM4-64 was observed. Data represent the mean  $\pm$  SE,  $n = 3$ .

domains gradually reappeared (Figure 4A). We hypothesized that this phenomena may be similar in mechanism to that of treatment with low concentrations of manu-A, and we expected that while heat shock may transiently suppress exocytosis, endocytosis would not be affected. To test this hypothesis, we analyzed the kinetics of exocytosis after heat shock (Figure 4B). As expected, exocytosis was attenuated and no release of acid phosphatase was observed 2 hr after the temperature shift. As a consequence, the concentration of released acid phosphatase was lower than that for the control cells (no temperature shift). In contrast, cellular uptake of FM4-64 was uninhibited by the temperature shift (Figure 4C). We therefore concluded that heat shock temporarily halts exocytosis, but not endocytosis, thereby facilitating the disappearance of sterol-rich membrane domains in the plasma membrane, similar in effect to manu-A treatment.

#### Sterol-Targeting Antibiotic-Resistant Cells Exhibit Defect in Exocytosis

Resistance to antibiotics can be the result of multiple mechanisms. Our emerging model suggested the possibility that cells may exhibit tolerance toward sterol-targeting antibiotics where a defect in exocytosis is present. To investigate this possibility, we first examined the secretion of acid phosphatase from ergosterol mutant cells. Knockout of the *erg2* gene or simultaneous deletion of the *erg31* and *erg32* genes in fission yeast is known to cause tolerance to sterol-targeting antibiotics (Iwaki et al., 2008). However, we could not detect any defects in acid phosphatase secretion (data not shown).

We next examined overexpression of the *SPCC23B6.04c* gene. We previously conducted genome-wide screening to identify genes conferring altered sensitivity to chemicals by their

overexpression (Nishimura et al., 2010). Among the  $\sim 4,800$  genes screened, *SPCC23B6.04c* was identified as a resistance gene common to AmB, nystatin, and TNM-F, a closely related congener of TNM-A (Matsunaga et al., 1989). We first investigated the cellular binding of filipin and TNM-AMCA to cells overexpressing *SPCC23B6.04c*. As expected, neither compound bound to the cells (Figures 5A and 5B), suggesting that antibiotic-sensitive sterol-rich membrane domains are not supplied to the plasma membrane in these cells. Next, we measured the degree of exocytosis and endocytosis. We found that the secretion of acid phosphatase was significantly decreased by overexpression of *SPCC23B6.04c* (Figure 5C). When overexpression was suppressed by addition of thiamine, this defect was not observed. In contrast, endocytosis was unaffected by overexpression of this gene (Figure 5D). The intensity of FM4-64 dye incorporated into these cells was no different to that of the control cells. Although the molecular function of the gene product of *SPCC23B6.04c* is still unknown, these results add further support to our model (discussed below, Figure 6).

#### Model for the Generation of Antibiotic-Sensitive Sterol-Rich Plasma Membrane Domains

Based on our results, we propose a model in which exocytosis supplies and endocytosis internalizes the specific membrane domains recognized by sterol-targeting antibiotics (Figure 6). In this study, we first showed that manu-A caused defects in membrane trafficking and abolishment of the effect of sterol-targeting antibiotics. Manu-A inhibited Cdc42 activity and its downstream event, exocytosis. In contrast, endocytosis was only partially inhibited. Heat shock and overexpression of a gene with unknown function, *SPCC23B6.04c*, induced similar defects in membrane trafficking and decreased binding of sterol-targeting antibiotics. BFA inhibited the incorporation of FM4-64, but not the secretion of acid phosphatase. Treatment with BFA exhibited intense fluorescence of filipin at the plasma membrane, suggesting that the selective inhibition of endocytosis resulted in the accumulation

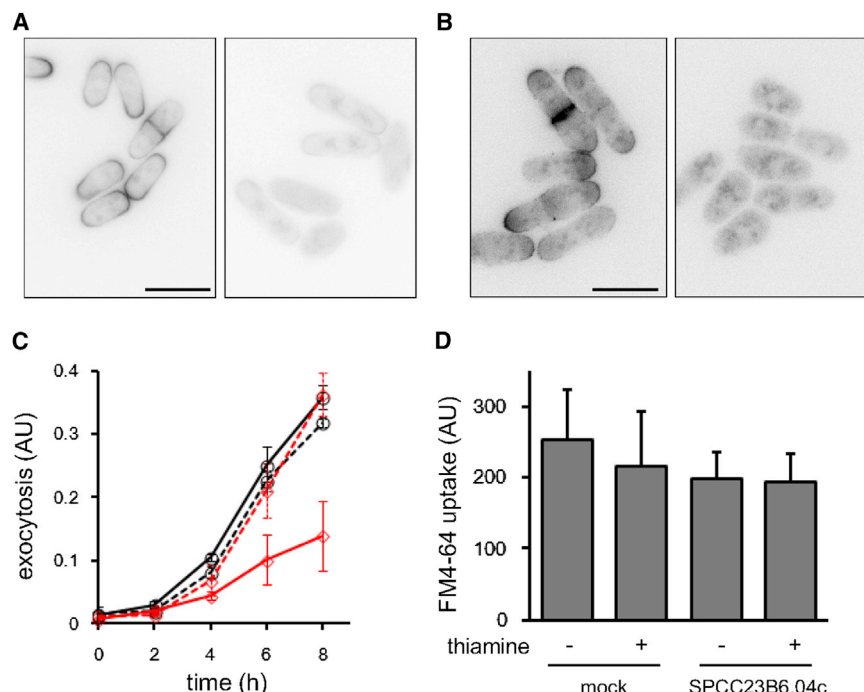


**Figure 5. Effect of Overexpression of SPCC23B6.04c on Sterol-Targeting Antibiotics and Membrane Trafficking**

(A and B) Binding of filipin (A) or TNM-AMCA (B) to control cells (left) and SPCC23B6.04c-overexpressing cells (right). Scale bars, 10  $\mu$ m.

(C) Attenuation of exocytosis by overexpressing SPCC23B6.04c. Activity of secreted acid phosphatase from control cells (black) and overexpressing cells (red) in the absence (solid) or presence (dashed) of thiamine was measured. Acid phosphatase activity was normalized with cell density. Cells were cultivated at 27°C. Error bars, SD, n = 3.

(D) Effect of overexpression of SPCC23B6.04c on endocytosis. Uptake of FM4-64 by control and overexpressing cells was observed. Error bars, SE, n = 3.

of excess sterols. Taken together, balanced membrane trafficking appears essential for the regulation of the quantity of antibiotic-sensitive and sterol-rich domains in the plasma membrane.

## SIGNIFICANCE

The species and quantity of lipid molecules in the plasma membrane are maintained by multiple mechanisms involving vesicle transport, lipid transport proteins, and local metabolic reactions (van Meer et al., 2008). Here, we have demonstrated that the proper balance between exocytosis and endocytosis produces membrane domains that are recognized by sterol-targeting antibiotics, as the specific inhibition of exocytosis, but not endocytosis by manu-A, heat shock, or overexpression of SPCC23B6.04c, all abolished the cellular binding of these antibiotics. Originally, membrane domains stainable by filipin were termed sterol-rich membrane domains (Wachtler et al., 2003), and similar staining patterns have since been observed when using fluorescently labeled TNMs (Nishimura et al., 2010). However, manu-A abolished the efficacy of not only filipin and TNMs, but also that of AmB, for which the subcellular localization remains unknown. Based on these observations, we suggest that the sterol-rich membrane domains are also intrinsically antibiotic-sensitive, at least in fission yeast. In silico simulations, based on experimental data, have predicted that the actin cytoskeleton, exocytosis, and endocytosis all coordinate to create cell polarity (Chou et al., 2012), which in turn is most likely regulated by Cdc42 (Mogilner et al., 2012). Many protein factors involved in cell polarization have been identified. However, mutations of these genes usually affect the total cell morphogenesis. Manu-A enables quick and complete inhibition of Cdc42 activity and

exocytosis, leading to the disappearance of sterol-rich antibiotic-sensitive membrane domains without the loss of cell shape polarity. This microbial metabolite could therefore prove a valuable tool for investigating the molecular mechanisms underlying the establishment and maintenance of cell morphogenesis.

## EXPERIMENTAL PROCEDURES

### Reagents

Filipin and AmB were purchased from Sigma-Aldrich. FM4-64 was from Invitrogen. TNM-AMCA was prepared as described previously (Ho et al., 2009). Manu-A was a gift from Kyowa Hakkō Kirin. Anti-GFP antibody (GF200) was purchased from Nacalai Tesque, and anti- $\alpha$ -tubulin antibody (B-5-1-2) was from Sigma-Aldrich.

### Yeast Strains

Deletion of the *cyp1* gene (SN246: *h<sup>-</sup> leu1-32 cyp1::kan<sup>r</sup>*) and *rho3* gene (SN168: *h<sup>-</sup> rho3::kan<sup>r</sup>*), and overexpression and tagging of Cdc42 were carried out as described in the Supplemental Experimental Procedures. An overexpression strain, SPCC23B6.04c, was constructed as previously reported (Matsuyama et al., 2006). Overexpression was induced in the absence of thiamine, whereas promoter activity was suppressed by the addition of thiamine (5  $\mu$ M). Other strains were gifts from various yeast researchers.

### Microscopy

Cells were treated with compounds at 27°C unless stated otherwise in the figure legends. Staining with filipin and TNM-AMCA were carried out as previously described (Nishimura et al., 2010; Wachtler et al., 2003). Vacuole morphology was visualized with FM4-64 as previously described (Gachet and Hyams, 2005). A MetaMorph system (Molecular Devices) was used for image acquisition together with an Olympus IX81 fluorescence microscope equipped with an UPLSAPO 100 $\times$  lens. Fluorescence intensity was quantified using the MetaMorph software.

### Extraction and Analysis of Sterols

Cells were cultivated in the presence or absence of manu-A, harvested, washed with ice-cold water, and stored at -80°C until extraction. Cells ( $\sim 3 \times 10^7$ ) were suspended in 75% aqueous MeOH (2 ml) containing 0.1% pyrogallol and 10  $\mu$ g 4,4'-di-tert-butyl-2,2'-bipyridyl as an internal control. CHCl<sub>3</sub> (1 ml) was added to the suspension, which was then vortexed vigorously (30 s).



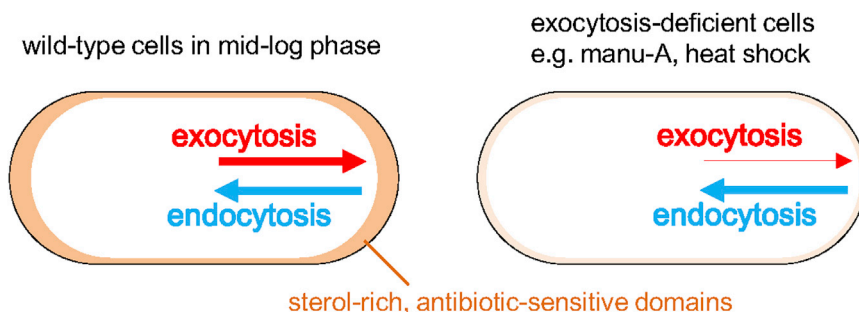


**Figure 6. Model of the Production of Sterol-Rich/Antibiotic-Sensitive Plasma Membrane Domains**

In actively dividing cells, exocytosis supplies sterol-rich and probably antibiotic-sensitive membrane domains to the plasma membrane. Endocytosis internalizes these domains. After the addition of manu-A or heat shock treatment, exocytosis is selectively suppressed while endocytosis is unaffected, leading to the disappearance of sterol-rich and antibiotic-sensitive membrane domains.

Petroleum ether (2 ml) was added to the mixture, followed by vortexing and centrifugation, and the upper layer was subsequently collected. This procedure was repeated twice to obtain three petroleum ether extracts. The extracts were pooled, dried over  $\text{Na}_2\text{SO}_4$ , and concentrated in vacuo. The pellet was dissolved in *N,N*-dimethylformamide (100  $\mu\text{l}$ ), and 2  $\mu\text{l}$  of this suspension was analyzed by high performance liquid chromatography (HPLC). The HPLC conditions were as follows: column, Shiseido Capcell Pak C18 UG120  $\phi$  4.6  $\times$  250 at 40°C; solvent system, 85%–100% MeOH over 20 min followed by 100% MeOH for 10 min with a flow rate of 1 ml/min; and detection, 282 nm. The quantity of ergosterol detected was calculated and normalized using the internal control.

#### Measurement of Acid Phosphatase Secretion

Acid phosphatase secretion was assayed as described previously with some modifications (Nakano et al., 2011; Wang et al., 2002). Cells grown overnight in YE5S media at 27°C were then cultivated at 27°C overnight in Edinburgh minimal medium (EMM) media. Cells were pelleted, washed with EMM without phosphate (EMMP), and suspended in fresh EMMP. Cell cultures (at an  $\text{OD}_{595}$  of 0.2) were incubated at 27°C with or without manu-A. At each time point, 500  $\mu\text{l}$  culture were centrifuged, and 400  $\mu\text{l}$  of the subsequent supernatant were added to 400  $\mu\text{l}$  substrate solution (2 mM *p*-nitrophenyl phosphate, 0.1 M sodium acetate, pH 4.0; prewarmed to 30°C), and the mixture was then incubated at 30°C for 5 min. Reactions were stopped by the addition of 400  $\mu\text{l}$  of 1 M NaOH. The absorbance at 405 nm was measured using the medium only as a blank control, and exocytosis efficiency was calculated as the ratio of  $\text{OD}_{405}/\text{OD}_{595}$ .

#### Statistical Analysis

Results are shown as mean values  $\pm$  SD or SE as indicated in the figure legends. Statistical significance was determined by Student's *t* test.

#### SUPPLEMENTAL INFORMATION

Supplemental Information includes Supplemental Experimental Procedures and six figures and can be found with this article online at <http://dx.doi.org/10.1016/j.chembiol.2014.10.014>.

#### ACKNOWLEDGMENTS

We thank Kyowa Hakko Kirin for the kind gift of manu-A. We are grateful to J. Ishiguro (Konan University) for the *act1/cps8* mutant strain and M. Yamamoto (The University of Tokyo) for the *pob1* mutant strain, both of which were provided through the Yeast Genetic Resource Center. We also thank R. Sugiura (Kinki University) for the *cpp1* mutant strain, H. Tatebe and K. Shiozaki (Nara Institute of Science and Technology) for the CRIB-expressing strain, M. Balasubramanian (Temasek Life Sciences Laboratory) for the lifeact-expressing strain, P. Pérez (Universidad de Salamanca) for the *cwg2* mutant strain, K.L. Gould (Vanderbilt University School of Medicine) for the *css1* mutant strain, and K. Takegawa (Kyushu University) for the ergosterol mutant strains. This work was supported in part by a Grant-in-Aid from the Japan Society for the Promotion of Science and the Ministry of Education, Culture, Sports, Science, and Technology of Japan.

Received: February 14, 2014

Revised: September 26, 2014

Accepted: October 30, 2014

Published: December 11, 2014

#### REFERENCES

- Arenz, C., Thutewohl, M., Block, O., Waldmann, H., Altenbach, H.J., and Giannis, A. (2001). Manumycin A and its analogues are irreversible inhibitors of neutral sphingomyelinase. *ChemBioChem* 2, 141–143.
- Bhuiyan, M.S., Ito, Y., Nakamura, A., Tanaka, N., Fujita, K., Fukui, H., and Takegawa, K. (1999). Nystatin effects on vacuolar function in *Saccharomyces cerevisiae*. *Biosci. Biotechnol. Biochem.* 63, 1075–1082.
- Boland, J. (1986). How do the polyene macrolide antibiotics affect the cellular membrane properties? *Biochim. Biophys. Acta* 864, 257–304.
- Breslow, D.K., Cameron, D.M., Collins, S.R., Schuldiner, M., Stewart-Ornstein, J., Newman, H.W., Braun, S., Madhani, H.D., Krogan, N.J., and Weissman, J.S. (2008). A comprehensive strategy enabling high-resolution functional analysis of the yeast genome. *Nat. Methods* 5, 711–718.
- Chou, C.S., Moore, T.I., Chang, S.D., Nie, Q., and Yi, T.M. (2012). Signaling regulated endocytosis and exocytosis lead to mating pheromone concentration dependent morphologies in yeast. *FEBS Lett.* 586, 4208–4214.
- Codlin, S., Haines, R.L., and Mole, S.E. (2008). btr1 affects endocytosis, polarization of sterol-rich membrane domains and polarized growth in *Schizosaccharomyces pombe*. *Traffic* 9, 936–950.
- Drabikowski, W., Lagwińska, E., and Sarzala, M.G. (1973). Filipin as a fluorescent probe for the location of cholesterol in the membranes of fragmented sarcoplasmic reticulum. *Biochim. Biophys. Acta* 291, 61–70.
- Espirito, R.A., Matsumori, N., Murata, M., Nishimura, S., Kakeya, H., Matsunaga, S., and Yoshida, M. (2013). Interaction between the marine sponge cyclic peptide theonellamide A and sterols in lipid bilayers as viewed by surface plasmon resonance and solid state  $^1\text{H}$  NMR. *Biochemistry* 52, 2410–2418.
- Estravis, M., Rincón, S.A., Santos, B., and Pérez, P. (2011). Cdc42 regulates multiple membrane traffic events in fission yeast. *Traffic* 12, 1744–1758.
- Fang, Y., Hu, L., Zhou, X., Jaiseng, W., Zhang, B., Takami, T., and Kuno, T. (2012). A genomewide screen in *Schizosaccharomyces pombe* for genes affecting the sensitivity of antifungal drugs that target ergosterol biosynthesis. *Antimicrob. Agents Chemother.* 56, 1949–1959.
- Gachet, Y., and Hyams, J.S. (2005). Endocytosis in fission yeast is spatially associated with the actin cytoskeleton during polarised cell growth and cytokinesis. *J. Cell Sci.* 118, 4231–4242.
- Graham, T.R., Scott, P.A., and Emr, S.D. (1993). Brefeldin A reversibly blocks early but not late protein transport steps in the yeast secretory pathway. *EMBO J.* 12, 869–877.
- Gray, K.C., Palacios, D.S., Dailey, I., Endo, M.M., Uno, B.E., Wilcock, B.C., and Burke, M.D. (2012). Amphotericin primarily kills yeast by simply binding ergosterol. *Proc. Natl. Acad. Sci. USA* 109, 2234–2239.

- Hara, M., Akasaka, K., Akinaga, S., Okabe, M., Nakano, H., Gomez, R., Wood, D., Uh, M., and Tamanoi, F. (1993). Identification of Ras farnesyltransferase inhibitors by microbial screening. *Proc. Natl. Acad. Sci. USA* 90, 2281–2285.
- Hayles, J., and Nurse, P. (2001). A journey into space. *Nat. Rev. Mol. Cell Biol.* 2, 647–656.
- Ho, C.H., Magtanong, L., Barker, S.L., Gresham, D., Nishimura, S., Natarajan, P., Koh, J.L., Porter, J., Gray, C.A., Andersen, R.J., et al. (2009). A molecular barcoded yeast ORF library enables mode-of-action analysis of bioactive compounds. *Nat. Biotechnol.* 27, 369–377.
- Iwaki, T., Iefuji, H., Hiraga, Y., Hosomi, A., Morita, T., Giga-Hama, Y., and Takegawa, K. (2008). Multiple functions of ergosterol in the fission yeast *Schizosaccharomyces pombe*. *Microbiology* 154, 830–841.
- Klemm, R.W., Ejsing, C.S., Surma, M.A., Kaiser, H.J., Gerl, M.J., Sampaio, J.L., de Robillard, Q., Ferguson, C., Proszynski, T.J., Shevchenko, A., and Simons, K. (2009). Segregation of sphingolipids and sterols during formation of secretory vesicles at the trans-Golgi network. *J. Cell Biol.* 185, 601–612.
- Kovar, D.R., Sirotkin, V., and Lord, M. (2011). Three's company: the fission yeast actin cytoskeleton. *Trends Cell Biol.* 21, 177–187.
- Ma, Y., Kuno, T., Kita, A., Asayama, Y., and Sugiura, R. (2006). Rho2 is a target of the farnesyltransferase Cpp1 and acts upstream of Pmk1 mitogen-activated protein kinase signaling in fission yeast. *Mol. Biol. Cell* 17, 5028–5037.
- Martin, S.G., Rincón, S.A., Basu, R., Pérez, P., and Chang, F. (2007). Regulation of the formin for3p by cdc42p and bud6p. *Mol. Biol. Cell* 18, 4155–4167.
- Matsunaga, S., and Fusetani, N. (1995). Theonellamides A-E, cytotoxic bicyclic peptides, from a marine sponge *Theonella* sp. *J. Org. Chem.* 60, 1177–1181.
- Matsunaga, S., Fusetani, N., Hashimoto, K., and Walchli, M. (1989). Bioactive marine metabolites 0.26. Theonellamide F - a novel antifungal bicyclic peptide from a marine sponge *Theonella* sp. *J. Am. Chem. Soc.* 111, 2582–2588.
- Matsuyama, A., Arai, R., Yashiroda, Y., Shirai, A., Kamata, A., Sekido, S., Kobayashi, Y., Hashimoto, A., Hamamoto, M., Hiraoka, Y., et al. (2006). ORFeome cloning and global analysis of protein localization in the fission yeast *Schizosaccharomyces pombe*. *Nat. Biotechnol.* 24, 841–847.
- Mogilner, A., Allard, J., and Wollman, R. (2012). Cell polarity: quantitative modeling as a tool in cell biology. *Science* 336, 175–179.
- Muhlrad, D., and Parker, R. (1999). Aberrant mRNAs with extended 3' UTRs are substrates for rapid degradation by mRNA surveillance. *RNA* 5, 1299–1307.
- Nakano, K., Toya, M., Yoneda, A., Asami, Y., Yamashita, A., Kamasawa, N., Osumi, M., and Yamamoto, M. (2011). Pob1 ensures cylindrical cell shape by coupling two distinct rho signaling events during secretory vesicle targeting. *Traffic* 12, 726–739.
- Nishimura, S., Arita, Y., Honda, M., Iwamoto, K., Matsuyama, A., Shirai, A., Kawasaki, H., Kakeya, H., Kobayashi, T., Matsunaga, S., and Yoshida, M. (2010). Marine antifungal theonellamides target 3 $\beta$ -hydroxysterol to activate Rho1 signaling. *Nat. Chem. Biol.* 6, 519–526.
- Nishimura, S., Ishii, K., Iwamoto, K., Arita, Y., Matsunaga, S., Ohno-Iwashita, Y., Sato, S.B., Kakeya, H., Kobayashi, T., and Yoshida, M. (2013). Visualization of sterol-rich membrane domains with fluorescently-labeled theonellamides. *PLoS ONE* 8, e83716.
- Park, H.O., and Bi, E. (2007). Central roles of small GTPases in the development of cell polarity in yeast and beyond. *Microbiol. Mol. Biol. Rev.* 71, 48–96.
- Perez, P., and Rincón, S.A. (2010). Rho GTPases: regulation of cell polarity and growth in yeasts. *Biochem. J.* 426, 243–253.
- Rincón, S.A., Ye, Y., Villar-Tajadura, M.A., Santos, B., Martin, S.G., and Pérez, P. (2009). Pob1 participates in the Cdc42 regulation of fission yeast actin cytoskeleton. *Mol. Biol. Cell* 20, 4390–4399.
- Simons, K., and Ikonen, E. (1997). Functional rafts in cell membranes. *Nature* 387, 569–572.
- Takeda, T., and Chang, F. (2005). Role of fission yeast myosin I in organization of sterol-rich membrane domains. *Curr. Biol.* 15, 1331–1336.
- Takeda, T., Kawate, T., and Chang, F. (2004). Organization of a sterol-rich membrane domain by cdc15p during cytokinesis in fission yeast. *Nat. Cell Biol.* 6, 1142–1144.
- Tanaka, T., Tsukuda, E., Uosaki, Y., and Matsuda, Y. (1996). EI-1511-3, -5 and EI-1625-2, novel interleukin-1 beta converting enzyme inhibitors produced by *Streptomyces* sp. E-1511 and E-1625. III. Biochemical properties of EI-1511-3, -5 and EI-1625-2. *J. Antibiot. (Tokyo)* 49, 1085–1090.
- Tatebe, H., Nakano, K., Maximo, R., and Shiozaki, K. (2008). Pom1 DYRK regulates localization of the Rga4 GAP to ensure bipolar activation of Cdc42 in fission yeast. *Curr. Biol.* 18, 322–330.
- Trajkovic, K., Hsu, C., Chiantia, S., Rajendran, L., Wenzel, D., Wieland, F., Schwill, P., Brügger, B., and Simons, M. (2008). Ceramide triggers budding of exosome vesicles into multivesicular endosomes. *Science* 319, 1244–1247.
- van Meer, G., Voelker, D.R., and Feigenson, G.W. (2008). Membrane lipids: where they are and how they behave. *Nat. Rev. Mol. Cell Biol.* 9, 112–124.
- Verghese, J., Abrams, J., Wang, Y., and Morano, K.A. (2012). Biology of the heat shock response and protein chaperones: budding yeast (*Saccharomyces cerevisiae*) as a model system. *Microbiol. Mol. Biol. Rev.* 76, 115–158.
- Volmer, A.A., Szpilman, A.M., and Carreira, E.M. (2010). Synthesis and biological evaluation of amphotericin B derivatives. *Nat. Prod. Rep.* 27, 1329–1349.
- Wachtler, V., Rajagopalan, S., and Balasubramanian, M.K. (2003). Sterol-rich plasma membrane domains in the fission yeast *Schizosaccharomyces pombe*. *J. Cell Sci.* 116, 867–874.
- Wang, H., Tang, X., Liu, J., Trautmann, S., Balasundaram, D., McCollum, D., and Balasubramanian, M.K. (2002). The multiprotein exocyst complex is essential for cell separation in *Schizosaccharomyces pombe*. *Mol. Biol. Cell* 13, 515–529.
- Wang, H., Tang, X., and Balasubramanian, M.K. (2003). Rho3p regulates cell separation by modulating exocyst function in *Schizosaccharomyces pombe*. *Genetics* 164, 1323–1331.
- Yan, Z., Costanzo, M., Heisler, L.E., Paw, J., Kaper, F., Andrews, B.J., Boone, C., Giaever, G., and Nislow, C. (2008). Yeast Barcoders: a chemogenomic application of a universal donor-strain collection carrying bar-code identifiers. *Nat. Methods* 5, 719–725.
- Yang, W., Urano, J., and Tamanoi, F. (2000). Protein farnesylation is critical for maintaining normal cell morphology and canavanine resistance in *Schizosaccharomyces pombe*. *J. Biol. Chem.* 275, 429–438.
- Zeeck, A., Schröder, K., Frobel, K., Grote, R., and Thiericke, R. (1987). The structure of manumycin. I. Characterization, structure elucidation and biological activity. *J. Antibiot.* 40, 1530–1540.